Energy Equip. Sys./ Vol. 6/No. 4/Dec. 2018/ 393-412

ENERGY EQUIPSYS

Energy Equipment and Systems

http://energyequipsys.ut.ac.ir
www.energyequipsys.com

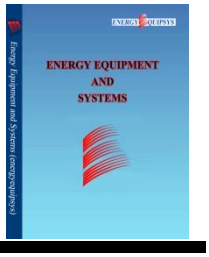

Study of flow and heat transfer characteristics in a periodic zigzag channel for cooling of polymer electrolyte fuel cells

Author

Elham Kazemi [a]
Alireza Shateri [a*]

[a] Mechanical Engineering Department, Shahrekord University, Shahrekord, Iran

ABSTRACT

In this study, a periodic zigzag channel with rectangular cross-section has been used in order to obtain a high-efficiency system for cooling a polymer electrolyte fuel cell. An appropriate function of fuel cells and enhancement of their lifetime require uniform temperature conditions of around 80°C. On the other hand, due to volume and weight constraints, a low-density compact heat exchanger is required, where the coolant fluid is water and the flow regime is laminar with a Reynolds number of 200. In order to consider these problems and increase the heat transfer rate under these conditions, a three-dimensional periodic zigzag channel is employed and the results are compared with the results which have been obtained for the straight channel. The results indicate that the zigzag channel generates chaotic advection and provides a good mixture of the hot fluid adjacent to the wall and the cool fluid away from it. This leads to a uniform temperature distribution along the channel. In addition, the values of Nusselt number and friction coefficient show that average Nusselt number in the zigzag channel is 6.5 times larger than that in the straight channel while the pressure drop remains approximately constant.

Article history:

Received : 02 March 2018
Accepted : 07 May 2018

Keywords: PEM Fuel Cell, Heat Transfer, Chaotic Advection, Zigzag Channel.

1. Introduction

Fuel cells are among the newest energy exchangers that converge the chemical energy of fuel to electrical energy and heat through electrochemical reactions. Fuel cells are of many types, among which, polymer membrane fuel cells have attracted more attention due to their lower volumes, higher initializing speeds and lower operating temperatures. In addition, due to the fact that water vapor is the only material which is resulting from the electrochemical reactions in this cell, it does not have environmental effects and is considered as a clean energy source. This fuel cell can be used in the transportation industry, automotive industry, mobile industry, mobile power supplies, spacecraft, power generation and so on [1-3].

The efficiency of the fuel cell is about 50%, that is, heat is generated just as much as the electrical energy is generated in the cell [4]. Therefore, thermal control of fuel cell is one of the important factors to improve its performance. The temperature above the working temperature and the non-uniformity of temperature along the cell are two important factors to reduce the efficiency and destruct the hardware of the cell which is resulting in its shorter life span.

* Corresponding author: Alireza Shateri
Mechanical Engineering Department, Shahrekord University, Shahrekord, Iran
Email: Shateri@eng.sku.ac.ir

The common cooling channels which have been used in fuel cells are straight. The streamlines of the fluid in them are direct leads to very little mixing in the fluid and low efficient heat transfer. In addition, as the boundary layer along the straight channel grows, the heat transfer will be reduced and very hot points will be created at the cell. Therefore, it is inevitable to use a channel that can increase fluid mixing while keep the pumping costs at a reasonable level and have a relatively simple structure.

Researchers have examined different models for fulfilling the aforementioned conditions in recent years. Chen et al. [3] developed six cooling models, including three spiral models and three parallel models, for analyzing and finding an optimal cooling model, between solid plates and coolant fluids in a fuel cell. In spiral geometries, the flow enters the channel from one point and gets out in the opposite point after passing through the spiral path, which has been designed in three different models, so that the entry and exit points are the points of the two heads of one of plate diameters .In parallel geometries, the flow is divided into two branches in the inlet and passes through parallel or spiral paths which have been presented in three different designs, and then two branches of the flow are interconnected and extruded on the other side of the plate. The results showed that the spiral model has a better cooling than parallel models. There is greater temperature uniformity and lower maximum temperature, particularly in the second and third spiral models, which are modified versions of the first model. The reason for this is the poor distribution of the cooling fluid in parallel models in comparison to spiral models. However, the pressure drop of spiral models is higher than that of parallel ones. The authors concluded that finding an optimal relationship between pressure drop and appropriate cooling needs further research.

Choi et al. [5] also examined six geometries for PEM fuel cell cooling channels including three spiral and three parallel models. The spiral geometries which have been examined in their study were the geometries that were presented by Chen et al. [3]. Parallel geometries were also included the major presented model and two new models. In one of the new parallel models, the flow was divided into two branches after it entered the channel, and the two branches conjoined and the flow got out of the opposite vertex point (the other side of the plate diameter) before it got out of the cooling channel. In the other parallel geometry, the flow was divided into three branches after entering the plate and passing along its width, and three branches of the flow conjoined after passing through the spiral path at the adjacent vertex of the inlet point, and got out after passing through the plate width, from the opposite entrance point which has been located on the other side of the plate. The results of this study showed that among the examined models in this study, the third spiral model (in which the flow has a spiral path between the inlet and outlet points) and the third parallel model (in which the flow was distributed among three branches and passed through a spiral path) had a better cooling performance. However, the cooling performance of the spiral model was better than that of the parallel model in terms of control of the maximum surface temperature and uniformity of temperature. This difference becomes more evident in performance when the heat flux increases. But the spiral model has greater pressure drop due to higher velocity of the fluid and because of having more bends.

Yu et al. [6] used the Multi-Pass Serpentine Flow-Field (MPSFF) to find the best model in thermal control of cooling plates. Their findings showed that, considering the two factors of uniformity and maximum temperature, the Multi-Pass Serpentine Flow-Field (MPSFF) geometry has better cooling operation than ordinary spiral models, although its pressure drop is higher in a specific Reynolds number.

Since different parallel and spiral models failed to improve both the heat transfer and pressure drop conditions simultaneously, the researchers studied channels, while having a simpler geometry and a consequent lower pressure drop, that could create a good mixing for hot and cold fluid particles and increase heat transfer. This will be possible with the help of secondary flows. Thus, researchers have focused their attention to channels in which a secondary flow is created. These flows were first reported in curved tubes [7]. Researchers reported the formation of a secondary flow in other spiral channels in later years. Wang and Liu [8] reported the creation of a secondary flow in micro-channels with square cross-sections. Their numerical results showed that the secondary flow increases the pressure drop to some extent, but there is a much higher heat transfer.

The reason for the more significant increase in heat transfer than in pressure drop in these flows is the phenomenon which has been first

introduced by Aref as "chaotic advection" or "Lagrangian turbulence" [9]. Chaotic advection in a laminar flow is created by simple geometric deviation, but the motion of particles is such that each particle passes through a completely different direction from its adjacent particles. In addition, particle elements get stretched and folded along the path, that is resulting in a higher particles contact and a better heat transfer. All of these factors help to provide better conditions for heat transfer in a microscopic view. However, since the geometric shape of the channel is not so complicated and the flow regime is laminar, the pressure drop is not high. Considering that this issue is very important from the point of view of heat transfer and cooling of electronic components, various experimental studies and numerical simulations have been carried out in recent years to find this type of geometry. Investigations showed that the path of the particles will be chaotic if a plate flow is exposed to a periodic deviation in the boundary. In addition, the range of the Reynolds number ,which will create a chaotic advection, has been presented for each of geometries in the laminar flow [10].

Acharya et al. [11] investigated the effect of chaotic mixing on heat transfer numerically and experimentally by modifying the geometry of spiral exchangers. The studied exchanger in this research was a spiral channel with a coiled circular cross sections the axis of which was periodically rotated under a 90 ° angle. They showed that the temperature profile became more uniform and the heat transfer increased due to chaotic mixing.

Mokrani et al. [12] investigated the effect of chaotic mixing on heat transfer by manufacturing two chaotic and spiral heat exchangers. The spiral exchanger was a coiled exchanger made of 90 ° bends, and the chaotic exchanger was also a coil that was created by twisting each bend under a ± 90 ° angle in relation to the previous bend. The results showed that heat transfer in chaotic heat exchangers has been improved by 13% to 27%.

Plate models are more preferable among the models that have been introduced to generate chaotic advection and secondary flow, because they can be used as compact or plate heat exchangers in various industries. Considering that the flow in the micro channels has a laminar regime and mixing of the two fluids as well as the heat transfer occurs so slowly, Xia et al. [13] used a geometry in the chemical industry that led to chaotic advection (Fig. 1a) in a microstructure reactor. The simulation results proved the formation of chaotic flow and showed that the channel, in addition to increasing the reaction speed versus the straight channel, also providing a better cooling effect in a exothermic reaction.

Senn and Poulikakos [14] numerically studied the Laminar mixing, heat transfer and pressure drop in a tree micro channel net with T-shaped branches (Fig. 1b), and assessed the feasibility use of it in PEM fuel cell cooling by comparing the results with the common spiral channel. Their findings showed the formation of secondary flows and Laminar mixing along the channel. A tree network of six branch levels, in addition to having a higher heat transfer capacity, has a pressure drop equal to half the pressure drop of the spiral network with the same inlet surface and Reynolds number.

Another factor that causes chaotic advection is the presence of barriers in the fluid path. Kuo et al. [15] investigated the effects of various barriers on the wall of Polymer electrolyte fuel cell flow channels in a laminar flow at Reynolds number of 200. These barriers were wavy, trapezoid and ladder shaped. The numerical simulation results for the two-dimensional model showed that the Nusselt number almost doubles in these channels in comparison to the straight channel.

By pointing out the importance of PEM fuel cell cooling systems and the volume limitation and the necessity of reducing the electrical resistance of the bipolar plates, Lasbet et al. [4] proposed the use of the C-shaped channel (Fig. 1-c), which was first introduced by Liu et al. [16] and which led to chaotic mixing, in order to increase the current density. The numerical results showed that the heat transfer coefficient of this type of channel is approximately 6 times of the straight channel with the same section level. Although the pressure drop is higher in

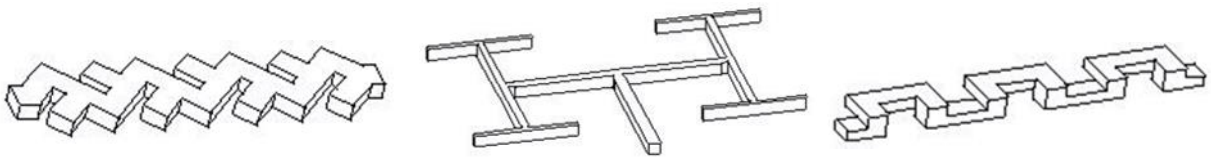

(a) (b) (c)

Fig.1. A few chaotic geometries

this channel than that of straight channel, the ratio of the coefficient of friction to the Nusselt number is less, which is indicating a higher heat transfer relative to the pressure drop.

Gupta et al. [17] studied laminar flow and heat transfer in a periodic trapezoidal channel with triangular cross-section. They compared the heat transfer and pressure drop changes between flow in square, circular and semi-circular sections and triangular cross section. In the flow at Reynolds numbers less than 200, the results showed that the triangular cross section has the optimum mode in terms of heat transfer and pressure drop. The authors attributed this result to the formulation of Dean Vortices.

Sui et al. [18, 19] numerically simulated the fully developed flow with a rectangular cross section in a periodic wavy channel. Their findings showed that when the flow of the cooling fluid passes through the bending points of the channel, secondary flows (Dean Vortices) are formed and their patterns are changed along the flow. This result in chaotic advection greatly increases the mixing of fluid and heat transfer. However, the increase in pressure drop due to mixing is less than the increase in heat transfer in comparison to the straight channel with the same section area.

Mangeaud et al. [20] used the two-dimensional Zigzag channel in order to examine the mixing of two different chemical species, showed that chaotic advection occurs at Reynolds above 80. Additionally, in a given Reynolds number, there is an optimal relationship between the length of the periodicity and the width of the channel. However, since the results of Mangeaud et al. were based on a two-dimensional model, they were incapable of examining the flow in the cross section and Dean Vortices.

Zheng et al. [21] investigated the simulation of transient laminar heat transfer in periodic zigzag channels. The laminar flow in wavy channels is unsteady at sufficiently large Reynolds numbers. This study examined a computational fluid dynamics method to study the transient laminar flow and heat transfer in an intermittent zigzag channel with a semicircular cross-section. The computational range comprised seven repetitive zigzag units. The Reynolds number ranged from 400 to 800 and the Prandtl numbers ranged from 0.7 to 20 with the boundary conditions of the constant heat flux and constant wall temperature. The simulation results showed the fully developed flow after three replication units. In the transient regime, significant progress in the heat transfer rate was observed to occur in exchange to a lower increase in the pressure drop. Both of these cases increase as the Reynolds number increases. Moreover, the structure of Vortices was simulated at different times and different Reynolds numbers and it was observed that an increase in the Reynolds number will lead to Vortices with smaller scale length that play a major role in increasing the heat transfer rate.

Zheng et al. [22] investigated the chaotic advection for a laminar and steady flow and heat transfer in zigzag channel with square cross-section. Flow simulations for different Reynolds numbers ranging from 50 to 400 showed that, initially the flow is intermittent, and then, as the Reynolds number increases, secondary flows are formed and the flow becomes chaotic. As a result, heat transfer and pressure drop are both increased.

Vinsard et al. [23] investigated chaotic advection and heat transfer in two similar two-dimensional periodic flows and their corresponding three-dimensional periodic flow. Chaotic advection can effectively increase the heat transfer rate between boundaries and fluids with high Prandtl numbers. These fluids are usually very viscous, and therefore the creation of a turbulent flow is not a satisfactory solution, because the energy which has been needed to mix the flow will be too costly. This study also examined the flow between two non-centered rotary cylinders and two co-centered ovals, it showed that chaotic heat transfer increases during each periodicity with the advection of the position of the saddle point.

Anxionnaz-Minvielle et al. [24] examined the application of chaotic advection for viscous fluids in heat exchangers/reactors. For viscous fluids, laminar hydraulic conditions and intensified heat and mass transfer are opposite phenomena. This study examined channel geometry experimentally based on the split and re-combine pattern. This chaotic structure was used to ensure heat and mass transfer. In this regard, the efficiency of the energy of heat exchangers and various reactors which are having this pattern was evaluated and the overall performance of these plate exchangers was compared with the folded pattern. The results showed that the efficiency of the energy of this geometry increases more in the case of more viscous fluids than in the case folded

geometries due to the balance between the diffusion mechanism and advection. In addition, the energy efficiency of chaotic geometry appears at Reynolds numbers less than 50.

Bahiraei et al. [25] studied the effect of chaotic advection in a laminar flow for a non-Newtonian nanofluid which is containing TiO_2 nanoparticles. For this purpose, they compared the hydrographic properties of nanoparticles in a C-shaped channel with the straight channel. They showed the heat transfer and pressure drop is higher in the C-shaped channel than in the straight channel, which is due to the effective mixing of the C-shaped channel as a result of chaotic advection, that is resulting in a more uniform profile of temperature and velocity in this channel. In addition, the use of nanofluid in both channels shows better cooling results and higher pressure drop. In the small Reynolds numbers, the development of chaotic flow leads to a greater increase in heat transfer than the required pumping power. In addition, the simultaneous use of nanoparticles and chaotic advection leads to the increased efficiency of energy and non-precipitation of nanoparticles.

Considering the importance of cooling the fuel cells and the necessity of designing a high-performance compact exchanger, a three-dimensional zigzag channel with rectangular cross-section has been used as a heat exchanger for cooling the fuel cell of the polymer membrane. The channel dimensions and hydrodynamic and thermal conditions are considered like the actual conditions in the fuel cell. Using the simulation results, the effect of secondary flows and chaotic advection are determined on heat transfer and pressure drop and the possibility of using this model is assessed in fuel cell technology.

Nomenclature

a	Half of the channel width (m)
A	Cross-sectional area of the channel (m^2)
b	Half of the channel depth (m)
C_f	Skin friction coefficient (-)
C_P	Specific heat capacity ($JKg^{-1} K^{-1}$)
D	Channel depth (m)
D_h	Hydraulic diameter (m)
f	Moody (or Darcy) friction
h	Heat transfer coefficient ($Wm^{-2} K^{-1}$)
K	Thermal conductivity ($Wm^{-1} K^{-1}$)
L	Channel length (m)
Nu	Nusslet number (hDh^{K-1})
P	pressure (Pa)
Pe	Peclet number ($\rho U \bar{D}_h C_p K^{-1}$)
Pr	Prandtl number ($\mu C_p K^{-1}$)
q"	Wall heat flux (Wm^{-2})
R	Ratio of linear length of the periodic step to channel width (S/W)
Re	Reynolds number ($\rho U \bar{D}_h \mu^{-1}$)
S	Linear length of the periodic step (m)
s	Curvilinear coordinate (m)
T	Temperature (K)
t	Time (s)
u	Velocity (ms^{-1})
W	Channel width (m)
x	x-coordinate (m)
y	y-coordinate (m)
z	z-coordinate (m)

Greek symbols

c	Thermal diffusivity
Δ	Difference (m^2s^{-1})
μ	Dynamic viscosity (Pa.s)
ρ	Fluid density (Kgm^3)

2. Computational model

2.1. Geometric model

The geometry under study, as schematically shown in Fig. 2, is a three-dimensional zigzag channel with a length of 80 mm. The corners in this channel have 90 ° angels. The cross sectional area of the channel is rectangular with a length to width ratio of 2 and a hydraulic diameter of 1.33 mm. The channel is 2 mm wide and 1 mm deep. As mentioned earlier, these values are similar to actual values in a fuel cell [4].

To find the best geometry of zigzag channel, the horizontal length of each zigzag unit, S, is defined as the variable parameter and it is considered four different values of 2, 4, 8, and 16 mm for the S period. Since the overall length of the channel is constant, the number of zigzag units for the aforementioned S values will be respectively 40, 20, 10, and 5.

For the sake of simplicity of the analysis, the ratio of the periodicity length to the channel width (R=S/W) is chosen as the optimization parameter. Thus, four different modes of R=1,

2, 4 and 8 (Fig. 3) are considered and the results are examined in each mode. For the sake of comparison, the straight channel is considered which represents the asymptotic state S (S → ∞).

2.2. Governing Equations

In this computational model, the fluid flow and heat transfer have been considered to be stable and three-dimensional. Water, as the coolant fluid, has been assumed to be incompressible with constant properties. The governing equations for flow, conservation of mass, momentum and energy are expressed as follows:

Continuity: (1)

$$\frac{\partial u_j}{\partial x_j} = 0$$

Momentum: (2)

$$u_j \frac{\partial u_i}{\partial x_j} = -\frac{\partial P}{\partial x_i} + \mu\left(\frac{\partial^2 u_i}{\partial x_j\, \partial x_j}\right)$$

$$, i = 1,2,3$$

Energy: (3)

$$\rho c_p\, u_j \frac{\partial T}{\partial x_j} = k\left(\frac{\partial^2 T}{\partial x_j \partial x_j}\right)$$

where u_i represents the velocity in the directions x, y and z; P represents pressure; T represents temperature; ρ represents density; c_p represents specific heat capacity; and k represents the thermal conductivity of the fluid.

In order to make the governing equations dimensionless, using the hydraulic diameter D_h of the channel in the longitudinal scale, the

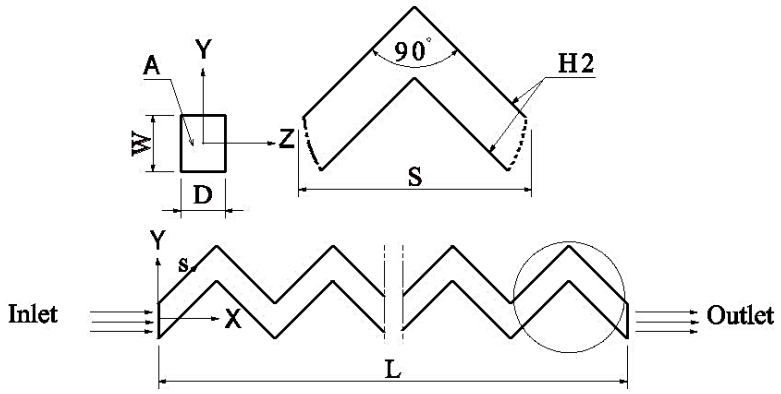

Fig.2. Zigzag Channel Specifications: W, width of the channel; D, depth; S, linear length of the periodic step; and L, total length of the channel

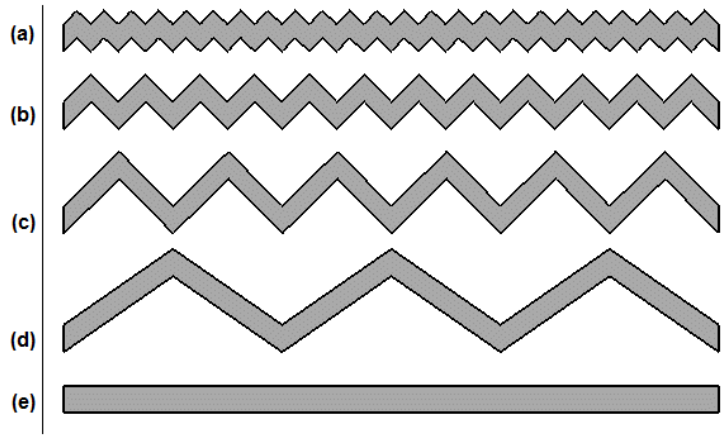

Fig.3. Different geometries of the zigzag channels (a) R = 1, (b) R = 2, (c) R = 4, (d) R = 8, and (e) R = ∞

average velocity U_m of the fluid in the velocity scale, and the input temperature T_{in} in the temperature scale are employed. Dimensionless parameters are defined as:

$$x_i^* \equiv \frac{x_i}{D_h}\ ,\ u_i^* \equiv \frac{u_i}{U_m}\ ,\quad T^* \equiv \frac{T - T_{in}}{\frac{q^{"} D_h}{k}}\quad ,\quad P^* \equiv \frac{P}{\rho U_m^2} \tag{4}$$

where x_i^* is dimensionless length in three directions, u_i^* is dimensionless velocity in three directions, T^* is dimensionless temperature, P^* is dimensionless pressure and $q^{"}$ is the wall heat flux.

Based on the above parameters, the dimensionless numbers of Reynolds, Prandtl, and Peklet are defined as follows::

$$Re = \frac{\rho U_m D_h}{\mu},\ Pr = \frac{C_p \mu}{k},\quad Pe = Re \times Pr \tag{5}$$

Using the aforementioned dimensionless parameters, the dimensionless equations are rewritten as follows:

Continuity: (6)

$$\frac{\partial u_j^*}{\partial x_j^*} = 0$$

Momentum: (7)

$$u_j^* \frac{\partial u_i^*}{\partial x_j^*} = -\frac{\partial P^*}{\partial x_i^*} + \frac{1}{Re}\left(\frac{\partial^2 u_i}{\partial x_j\, \partial x_j}\right)$$

Energy: (8)

$$u_j^* \frac{\partial T^*}{x_j^*} = \frac{1}{Pe}\left(\frac{\partial^2 T^*}{\partial x_j^*\, \partial x_j^*}\right)$$

2.3. Boundary conditions and numerical solution

The input flow is considered as fully developed in this problem, because due to the short length of the hydrodynamic input length in comparison to the length of the channel, we have ignored this length and only examined the extended length.

Therefore, the fully developed velocity profile has been assumed for the inlet velocity in rectangular cross-sections, which Marco and Han [26] obtained for a section with 2a and 2b dimensions, in such a way that the origin of the Cartesian coordinate system can be in the rectangular center, in the following way:

$$\frac{u}{u_{max}} = \left[1 - \left(\frac{z}{b}\right)^n\right]\left[1 - \left(\frac{y}{a}\right)^m\right] \tag{9}$$

$$\frac{u_{max}}{u_m} = \left(\frac{m+1}{m}\right)\left(\frac{n+1}{n}\right) \tag{10}$$

Natarajan & Lakshmanan [27] presented the following equations for m and n:

$$m = 1.7 + 0.5\ \alpha^{*-1.4} \tag{11}$$

$$\begin{cases} \mathrm{n} = 2 & \alpha^* \le \frac{1}{3} \\ \mathrm{n} = 2 + 0.3(\alpha^* - \frac{1}{3}) & \alpha^* > \frac{1}{3} \end{cases} \tag{12}$$

where $\alpha^* = b/a$. In this problem, a=1, and b=0.5, and consequently $\alpha^* = 0.5$. Thus, the following values are obtained for m and n:

$$\begin{cases} \mathrm{m} = 3.02 \\ n = 2.05 \end{cases}$$

The input fluid temperature is assumed to be uniformly T_{in}=298K.

The non-slip boundary condition and uniform wall heat flux condition apply on the walls of the channel.

The present PEM fuel cells generate a flux about 5000 w/m^2. However, q"=10Kw/m^2 has been used in the calculations ,considering the prediction of an increase in the power density in the future. [4].

The fixed pressure boundary condition has been applied in the output of the channel due to the fact that there is no developed flow. The laminar flow regime and the Reynolds number of 200 are considered to simulate the actual flow conditions in the fuel cell [4].

2.4. Grid independency

Three different hydraulic and thermal parameters, namely the maximum temperature along the channel, the difference in the wall temperature between the inlet and outlet, and the pressure drop across the channel are used to select the right grid. The results for the geometry with R=1 are shown in Table 1. As it can be seen, the quantities which examined in grids 6, 7 and 8 are not significantly different. Therefore, grid 6, with 1128271 nodes, is selected as the final grid. A similar process was followed for other geometries and the appropriate grid was selected for them.

Table 1. Examining three different factors for selecting the appropriate grid

$\Delta \mathbf{P}^{*}(-)$	$\Delta T(k)$	$T_{max}(k)$	**Node number**	**Grid**
62.47	16.30	311.34	212233	1
58.96	16.66	313.07	311896	2
56.30	17.58	314.87	487531	3
53.61	17.88	316.29	627936	4
55.84	17.96	315.88	829139	5
49.85	18.98	317.95	1128271	6
49.48	19.12	318.38	1593551	7
49.25	19.19	318.55	2003683	8

2.5. Validation

To evaluate the validity of the numerical results of the present problem, which indicates the thermal performance of the fuel cell of the polymer membrane, first this method is used to examine the thermal performance of the heat exchangers between the bipolar plates of the fuel cell. These heat exchangers were designed in such a way that the cooling fluid (water) can flow in a straight channel near the bipolar plates. The flow regime was laminar and the Reynolds number was about 200. The channel cross section is rectangular with a height of 1 mm and a hydraulic diameter of 1.33 mm, and the overall length of the channel is 8 cm. In these conditions, according to reference [4], a classical power-law decrease is observed in the Nusselt number, which has an asymptotic value of 3. This value corresponds to the values which have been presented in [28] and [29]. In addition, the average Nusselt number is 4.2 according to references [15] and [30], which corresponds well with the obtained values in this study. Furthermore, for the fully developed flow conditions in a straight channel, fRe is presented based on theoretical values and, according to the reference [4], has an asymptotic value of 62.2, which was also obtained as 60.92 in this research and it can be used as another proof for the accuracy of the results of this research. Tables 2 and 3 present a comparison of the Nusselt number and the friction coefficient which has been obtained in this study and other studies as well as the error percentage.

Table 2. Frictional coefficient in channel outlet and error percentage as compared with those in the references

Lasbet et al. [4]	**Current study**	
62.2	60.92	f Re
2.06	-	Error percentage

Table 3. The mean value of Nusselt number and the error percentage in comparison with the references

Kuo et al. [15] and Guo et al. [30]	**Current study**	
4.20	4.23	Nu
0.7	-	Error

3. Results

As mentioned earlier, chaotic advection in a laminar flow that caused by simple geometric deviation helps to provide better conditions in the microscopic view of heat transfer in a laminar flow. However, since the geometric shape of the channel is not so complicated and the flow regime is laminar, there is no great increase in the pressure drop. The noteworthy point here is that secondary flow is not efficient and effective for increasing the heat transfer by itself, because it only causes regular mixing. The difference between regular mixing and chaotic mixing is that regular mixing is due to the formation of a secondary motion in curved paths and in a laminar steady flow, which increases heat transfer. However, as the stream lines in the cross section plate include two secondary vortices and the path of the particles is closed curves, the particles in the vortex core are not mixed, but a periodic disturbance in the direction of fluid flow can make this secondary flow chaotic and, instead of closed paths, create spiral paths and achieve a higher degree of mixing [10]. A zigzag channel has been used in the present study which leads to chaotic advection [20]. Next, the existence of chaos in the flow is shown as a result of using the zigzag channel and its effect on the fluid, and then examines the heat transfer and pressure drop parameters in this channel in order to select the channel with optimal R ratio.

3.1. Chaos in the flow

A system is chaotic when satisfies any of the following conditions:

1- The flow is sensitive to initial conditions.
2- The flow leads to the stretching and folding of fluid particles.
3- The flow generates homoclinic or heteroclinic intersections.

In this paper, the condition of sensitivity to the initial conditions has been used to emphasize the chaotic flow of zigzag geometry. Sensitivity to the initial condition means that there are two different paths at the entrance to the channel for two particles with very little distance so that they diverge rapidly and get away from each other. In the straight channel, the input flow does not interfere with any barriers and does not change its direction up to the end of the channel, while the flow path is not steady in the zigzag channel and encounters numerous barriers up to the end and changes its direction. This causes the flow to be sensitive to the initial conditions in the zigzag channel, and the particles with close initial conditions pass through different paths due to geometric turbulences. For this purpose, two particles of fluid with close initial conditions have been traced in different models and their paths have been presented along the channel in Fig. 4.

As shown in Fig. 4, the paths of the particles in the straight channel is exactly the same and their distance remains constant until the end of the path. However, the path of the particles is different in the zigzag channels, and the distance of the particles is changing, although there are somewhat different conditions in the zigzag channel with R=1. In this channel, one of the particles is enclosed in a vortex in one of the corners, and after passing through a rotational path, continues the rest of the path in a zigzag track. The main difference in track of the particles in channel with R=1 and straight channel is the fluctuation of the flow lines in this zigzag channel. Therefore, it can be concluded that this channel is less chaotic than other zigzag channels, and the particles are not mixed in it correctly.

3.2. Mixing

The Poincare section is another means of expressing the characteristics of chaotic systems, which reduces the complexity of the problem by decreasing the dimension of the state space through the mapping of the flow. In the Poincare section, instead of recording the three-dimensional changes of the particle path with time, the particles' position is observed in a two-dimensional state. Like some other researchers [32, 33, 34, 35], this tool is used in this section in order to analyze fluid mixing and to show the non-diffusion advection in flow. The position of the particles is determined after the field of velocity becomes stable. The instantaneous position of each particle is obtained through time integration of its velocity at any given instant, based on the following equation:

$$x(t) = \int_0^t u(x(t'))dt' \tag{13}$$

where u represents the vector of velocity at the time, t and x represents the particle position vector. In this way, the path of each particl

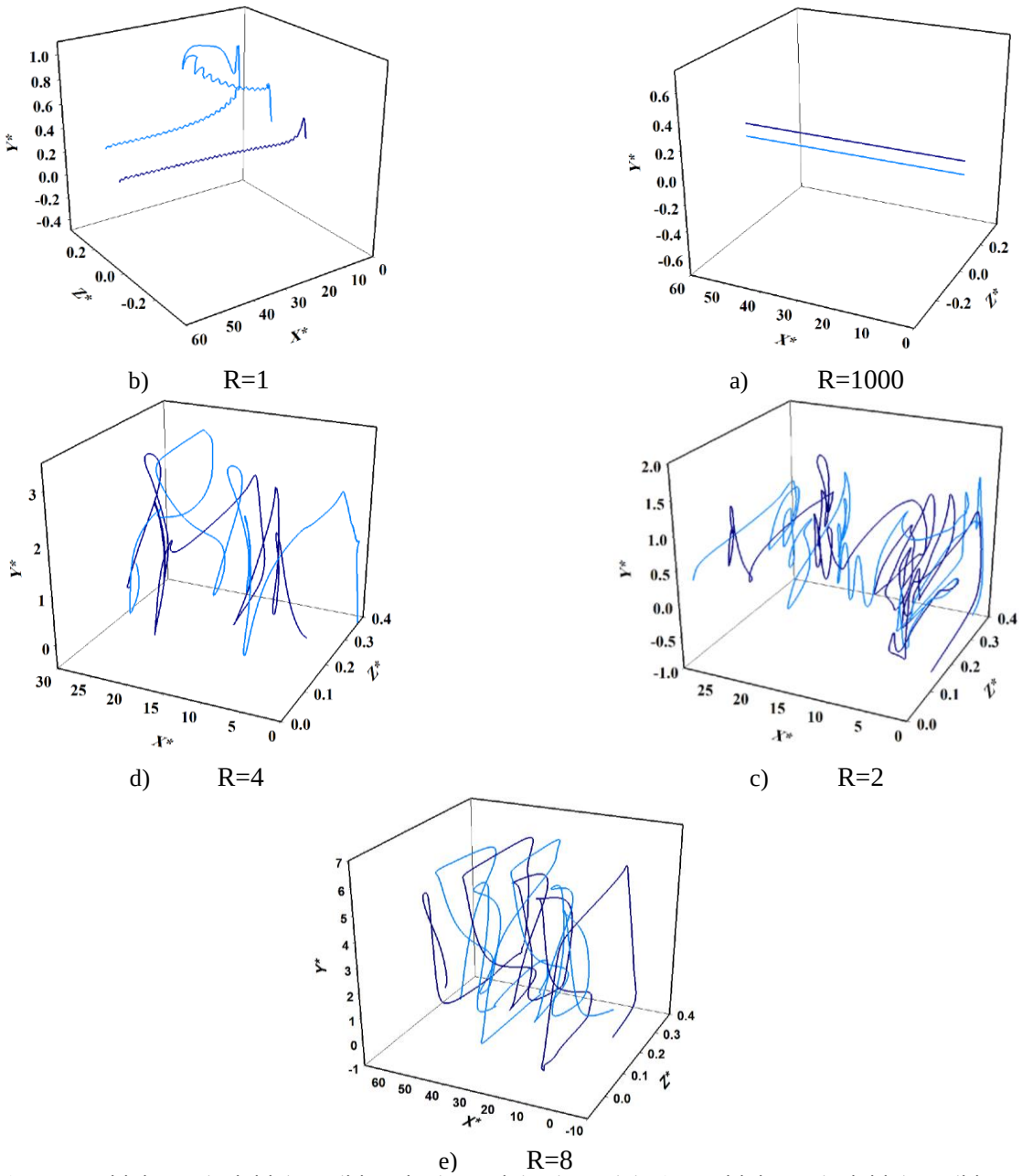

Fig.4. a) Not sensitivity to the initial conditions in the straight channel, b-e) Sensitivity to the initial conditions in the zigzag channels

can be plotted through the Lagrangian tracking of it.

For this purpose, 14 particles are traced on a half-diameter of the input rectangular of the zigzag channel with a ratio of R=2 with a distance of 0.05 from each other.. The Poincare section was created on the X-axis, as shown in Fig.5.

The effect of chaotic mechanism on the mixing of fluid particles is well observed in the Poincare section. By going through the channel, the particles lose their order and find a new position. Then they are separated from each other and dispersed all over a section. In other words, the accumulation and compaction of the points of contact of the particles' path and the Poincaré section are reduced and these points are scattered throughout the cross sectional area due to the exponential divergence of the particles in the chaotic flows. The particles along the channel traverse different paths due to the changes of paths

successively and the chaotic flow, and they are exponentially separated. This folding and stretching of the particle lines that rapidly occurs along the channel and causes the particles to spread in the section, is one of the signs of chaotic flows [33, 36]. As the paths are changed and the flow gets chaotic, the particles that were initially in a side by side position traverse different paths, which would increase the mixing.

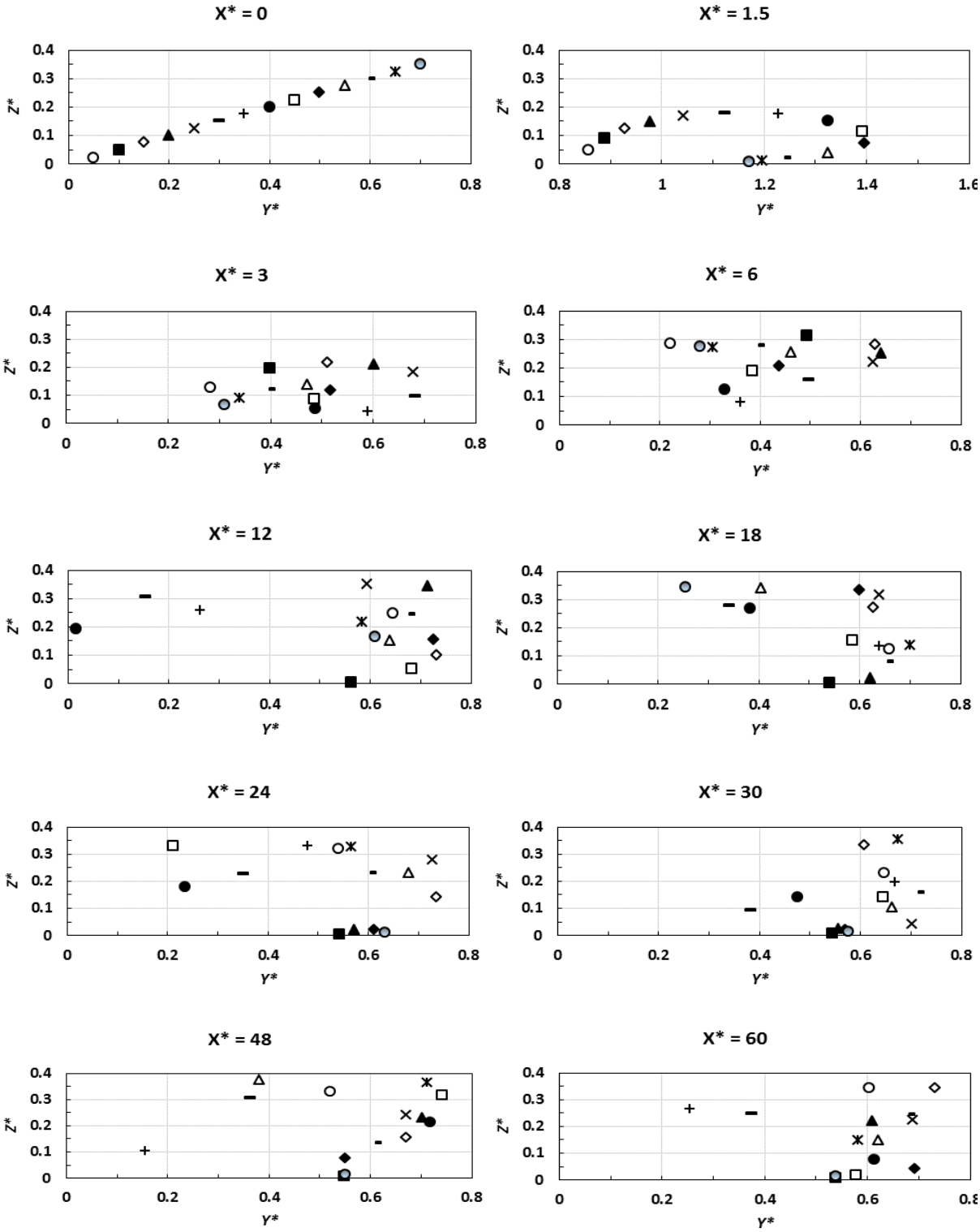

Fig.5. Poincare sections in the zigzag channel with R=2

3.3. Secondary flows

In the laminar flow inter-channel, the curvature's influence, albeit small, cannot be ignored. The curvature of the stream line causes secondary flows occur, which, when it was viewed in the cross section, includes a pair of rotating flow opposite to each other or roll-cells. These roll-cells were named Dean roll-cells after Dean [7] set forth the theory of this type of secondary flows [32]. In addition, the presence of sharp twists in a channel (for example, turnings with 90-degree angles) results in a periodic flow. The alternative repetition of these turnings escalates the Dean flow and leads to chaotic advection. Therefore, Dean Vortices are available in a flat channel with sharp twists. Dean Vortices lead to the stretching and folding of fluid elements and increasing heat transfer [33]. Aref [9] examined the problem of fluid motion in 1984 by analyzing the theory of one point Vortex in a two-dimensional model and concluded that if the position of a vortex alternately changes between two points, chaotic advection will be the result and finally good mixing will occur in the fluid.

The velocity field and temperature field are used in this study in order to study the formation of secondary flows and Dean Vortices. The velocity vectors in the cross section of the zigzag channels at a desired position (X*=48) are presented in Fig.6. This position is proportional to zigzag units 33, 17, 9 and 5, in channels with R=1, 2, 4, and 8, respectively. The study of the velocity field in all four types of zigzag channels shows the formation of a pair of Dean Vortices in the cross section. In the R=2 state, Dean Vortices have occupied more area of the cross section.

Figure 7 shows the temperature field at two successive sections of each channel. Fig. 7a shows the temperature field in the proximity of the inlet section of the straight channel (X*=12) and the proximity of the outlet channel of the straight channel (X*=48). As shown in the figure, the temperature is minimum in the central section of the channel and maximum in the vicinity of the walls and no mixing occurs in this channel. For zigzag channels, the temperature profile has been displayed in two successive cross sections, at the beginning and the end of a broken arm of the zigzag channel. As seen in the figure, the pattern and the position of the secondary flows are different at these two sections. Therefore, the changed pattern of flow between periodic zigzag units, as shown by Aref [9], is another reason to prove the chaotic advection in the present case.

A comparison of temperature which counters in zigzag channels in this study shows that the maximum temperature in the R=2 model is less and a more uniform temperature has been created in the whole section. In other words, the mixing has occurred well between the cool fluid of the channel center and the hot fluid adjacent to the channel wall.

3.4. Heat transfer

The local Nusselt number along the channel is calculated to examine the heat transfer characteristics in the zigzag channel. The Nusselt number depends on the position of the section in channel (x), according to the following equation:

$$Nu(x) = \frac{h(x)D_h}{k_f} \tag{14}$$

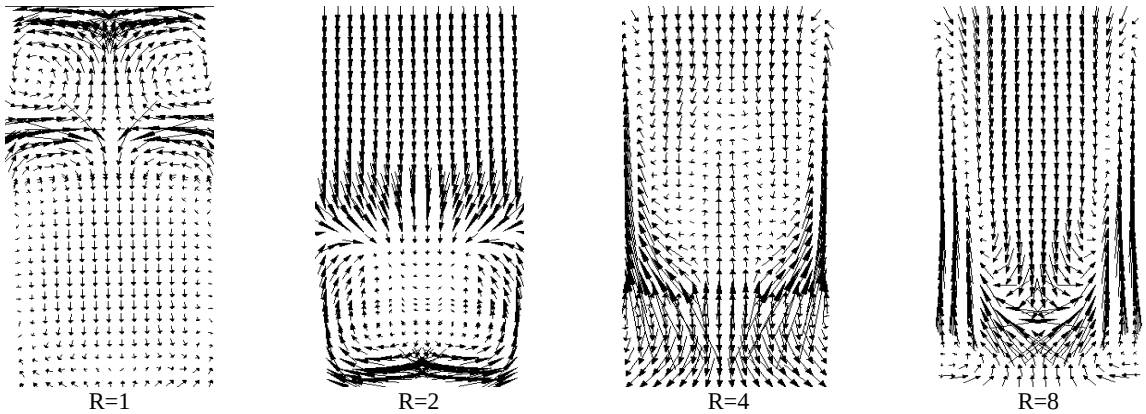

Fig.6. Velocity vectors and formation of secondary flows along cross sections of the zigzag channels at the x*= 48

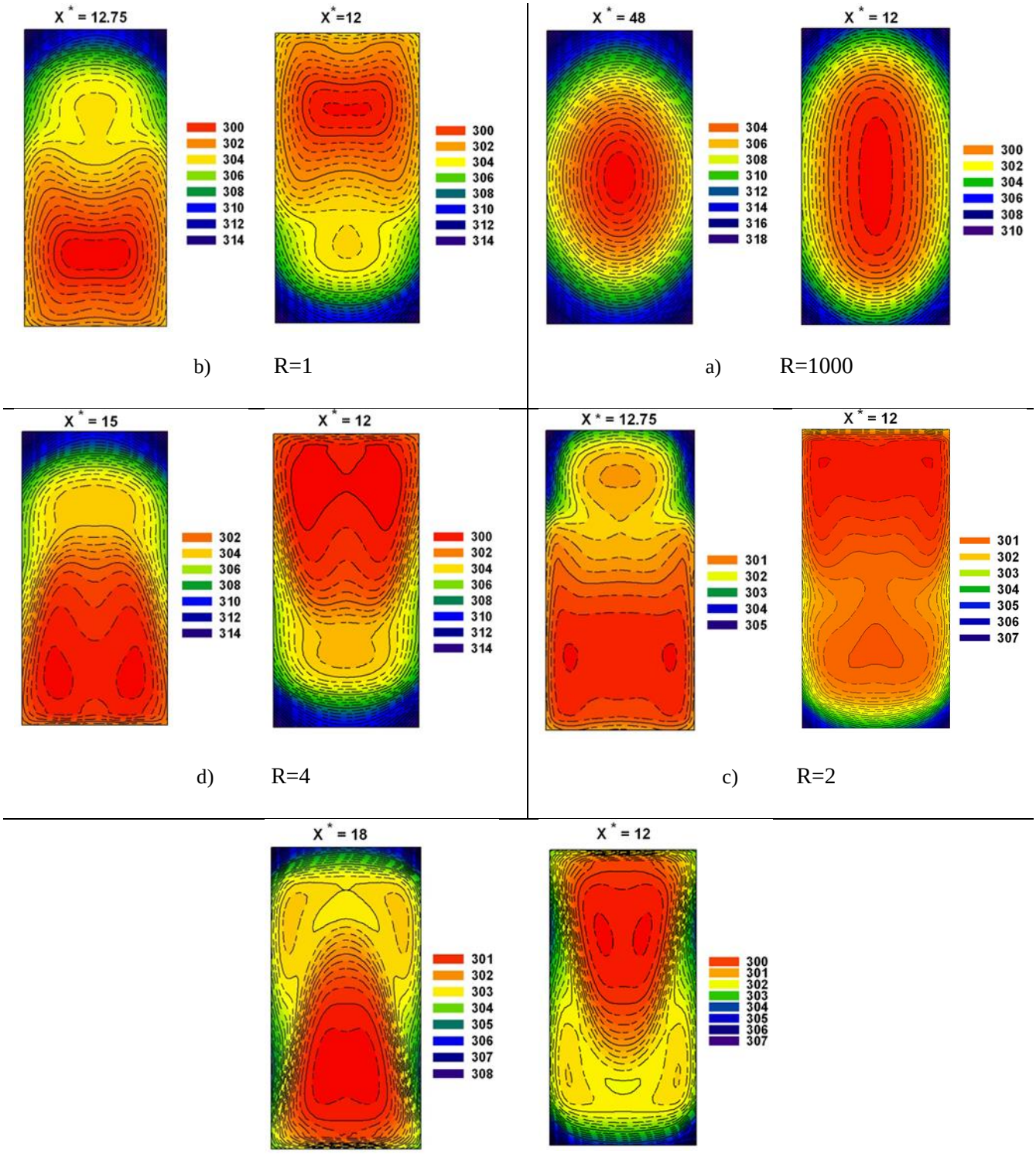

Fig.7. Isothermal contours at two different cross-sections in the length of each channel

The advection heat transfer coefficient is defined as:

$$h(x) = \frac{q^{"}}{T_{w,m}(x) - T_m(x)} \tag{15}$$

where $T_{w,m}$ represents the average temperature of the wall and T_m represents the average temperature at each section and they are obtained from the following equations:

$$T_{w,m}(x) = \frac{\int T\, ds}{s} \tag{16}$$

$$T_m(x) = \frac{\iint T\, dA}{A} \tag{17}$$

s represents the curvilinear coordinates on the channel wall and A represents the cross sectional area of the channel (Fig. 2).

Equations governing fluid flow and heat transfer, equations 6 to 8, were solved for four Zigzag channels of R=1, 2, 4, 8 as well as for the straight channel which were representing the limit state R → ∞. The flow conditions in all geometries are the same and like the actual flow conditions in fuel cells, have a laminar regime with a Reynolds number of 200 [4]. The Prandtl number of Pr=2.14 has been considered, which is related to water under 1 bar pressure and 80 ° C temperature conditions [31].

The Nusselt number graph are presented in Fig. 8 for zigzag geometries as well as the straight channel (R =1000). The heat transfer coefficient is high at the beginning of the channel due to the uniformity of the input temperature profile. However, with the growth of the thermal boundary layer, the heat transfer rate is reduced to an asymptotic value which is associated with the fully developed flow. But the flow in the zigzag channels does not undergo such a reduction and it is largely influenced by path fractures. The zigzag channels prevent the growth of the boundary layer and, due to having broken arms, cause the hydraulic flow of the boundary layer and, as a result, cause the thermal boundary layer to be destroyed and reformed.

Figure 8 shows that the Nusselt number has oscillating values across zigzag channels, and the maximum Nusselt number is observed after fractures due to changes in the flow and boundary layer in these areas.

The maximum values of the Nusselt number is related to the channel with the R=2 ratio, so that the average Nusselt number in this channel is higher than other R's. After a relative increase of up to about X*=15, the values of the Nusselt number in this channel have periodic changes with an average value of 26.6. In addition, the variation range in the values of the Nusselt number is around 14 in this channel, which is more than that in the other zigzag channels. The geometry with a ratio of R=4 is ranked in terms of the values of the Nusselt number after the channel with a ratio of R=2. The values of the Nusselt number in the R=4 geometry after an irregular process up to about X*= 10.5 have an average periodic process of 12.5 and a maximum value change of 9.7. The values of the Nusselt number have less variation range in geometry with a ratio of R=8 and its graph has been placed among the Nusselt number graph for R=4 geometry.

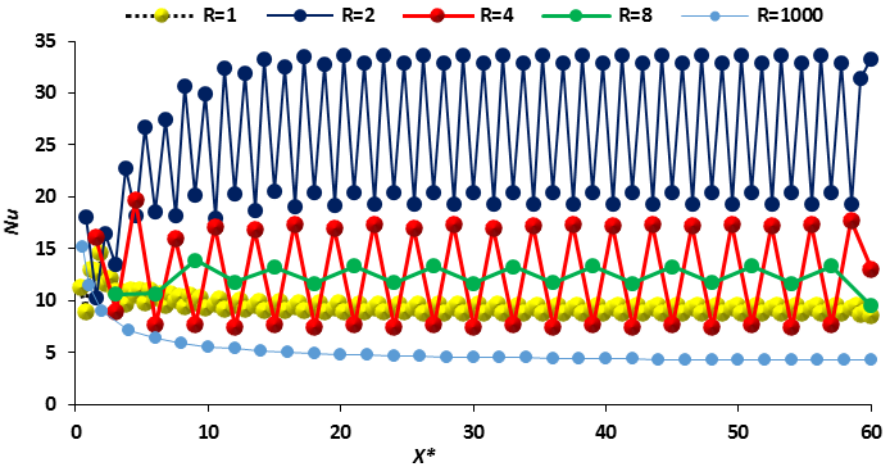

Fig.8. Evolution of the Nusselt number with the curvilinear coordinate for different channels

This is due to the prolonged flow path in the broken arms of the Zigzag channel due to the increased R-value, which is resulting in the damping of flow chaos between the two fractures.

The values of the Nusselt number from the X*=12 have undergone uniform oscillations with an average of 12.5 and a range of 1.5. As it is shown, the mean values of Nusselt are equal in the R= 4 and R=8 geometries. Finally, it is the graph of the R = 1 channel that is the variation range of the values of the Nusselt number of which lies in variation range of the values of the Nusselt number of the R=4 geometry. Moreover, the values of the Nusselt number in this geometry (R =1) are less than those in the R=8 geometry. This curve is flatter than the Nusselt curve in previous geometries and the variation range of the Nusselt number is about 0.9 in it. From X*=2, the average changes of this graph are similar to those of the straight channel graph. This is due to the fact that the distance of a greater volume of the fluid from the Geometric disturbances of the channel and their movement in a straight line. However, the effect of this geometry on the occurrence of chaos in the flow causes the average Nusselt number in this channel to be about 9.2, which is more than that in the straight channel, while the straight channel is about 4.2.

A general comparison of the graphs shows that the R=1 channel, despite a 2.2-time increase in the Nusselt number compared to the straight channel, has a closer proximity to it. The best thermal performance in the channel with R=2 occurs with a 6.5-time increase in the Nusselt number. With an increase in the R and the length of each period and hence the greater distance of channel fractures from each other, the fluid will find the opportunity to improve its disturbances. Therefore, the Nusselt number will increase less. However, in the two R=4 and R=8 channels, the Nusselt number is 3 times as much as the straight channel.

It should be noted that the oscillations of the Nusselt number would be damped due to a laminar mixing after a while if there was only one periodicity in the channel. But the repetition of this periodicity in a zigzag channel will keep the volatility of the Nusselt number. In total, the zigzag channel with any periodicity has a better thermal performance than the straight channel.

To examine the effect of flow chaos on the temperature profile in the cross section, the central section of the channel, i-e, X*=30, is randomly selected and plotted the temperature profile for all channels (Fig. 9). As it can be seen, the temperature profile is parabolic in the straight channel, and is at a higher level than the zigzag channels. In the straight channel, the temperature of particles of the fluid which are in the center of the channel is less than the temperature of the adjacent wall due to its distance from the walls and receipt of heat by the conduction method, while this has not been seen in the zigzag channels, because fluid particles rapidly diverge from each other in a chaotic flow, causing the successive stretching and folding of the fluid elements. As a result, the contact surface of the fluid elements has been increased and a better mixing has been occured. As the mixing of the flow improves,

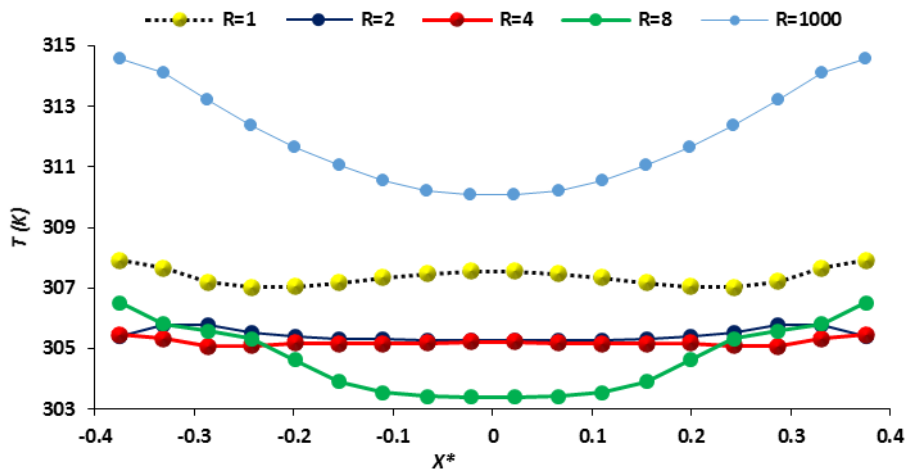

Fig.9. Temperature profile in the central cross section of the different channels (x*=30) (horizontal direction)

the cooler particles are shifted from the center of the channel to the warmer areas near the wall and the heat transfer process is increased. In this condition, the particles in a particular section of the channel have a more uniform temperature than the straight channel.

As shown in Fig. 9, the temperature profile is more uniform in the zigzag channels, and the minimum temperature does not occur in the center of the channel. The best state is related to the R =2 and R=4 models, which has a relatively flat profile. The effect of the formation of Dean Vortices (Fig. 6) is clearly seen in the temperature profile of the R=1 model, since the temperature profile graph for this geometry has two symmetric curves.

In general, it is known that heat transfer in a straight channel decreases in the direction of the flow, which can be attributed to the growth of the boundary layer and the uniformity of the flow. However, the formation of secondary flows increases the mixing of the fluid and increases the heat transfer in curved or broken channels. On the other hand, maximum temperature and temperature uniformity are two key factors in improving the performance and increasing the lifespan of fuel cells. The rise in temperature will accelerate the electrochemical reactions, which is resulting an increase in the speed of electrical current generation. Therefore, it is necessary to control the operating temperature at a certain maximum value and minimize this temperature in the entire channel in order to optimize the performance of the cell.

For this purpose, the index of temperature uniformity (IUT) is presented below and the design is done based on the minimum of this index.

$$IUT = \frac{\iiint |T_{x,y,z} - T_{ave}|\, dV}{V} \tag{18}$$

Another index which has been used to control the uniformity of temperature is $\Delta T = T_{max} - T_{min}$which T_{max} and $T_{min}$are the maximum and minimum surface temperatures along the channel, respectively. The cooling fluid channels in the cell should have a lower temperature difference (ΔT). Figure 10 presents two indices of temperature uniformity and minimum and the maximum temperature difference (ΔT) for different models in the column graph.

The maximum values of both indicators are shown in the R=1 model, which are indicating a lack of proper fluid mixing in this model. This can be justified due to the higher heat transfer surface in this model and use of the boundary condition of constant heat flux in all models. The R= 2 model is the most appropriate model in terms of both indices, after which lie the R=8 and R=4 models, respectively. The reason for this is the effect of the formation of secondary flows and Dean Vortices on the improvement of fluid mixing in the three recent models, with regard to what was mentioned in the previous sections.

3.5. Pressure drop

To examine the effect of different geometries on pressure drop, the coefficient of friction along the channel is presented in Fig. 11. The coefficient of friction at each section of the channel is calculated using the following equation:

$$f(x) = -\frac{\partial P_m}{\partial x}\frac{2D_h}{\rho U_m^2} \tag{19}$$

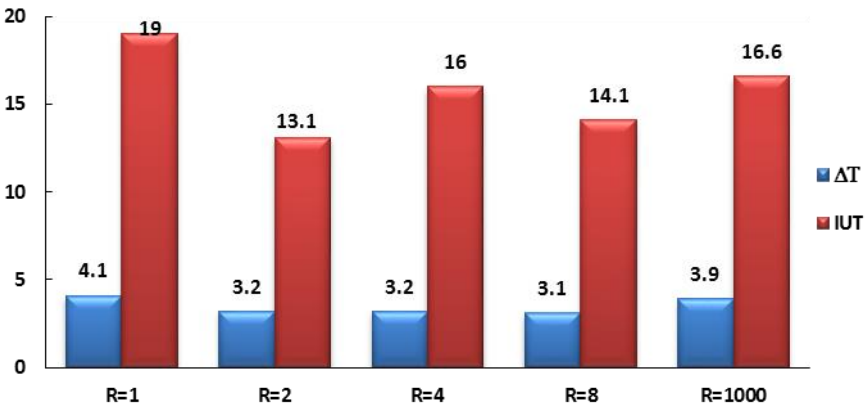

Fig.10. Temperature uniformity indexes for different channels

P_m the average static pressure at each level is defined as follows:

$$P_m(x) = \frac{\iint P\, dA}{A} \tag{20}$$

Regarding the use of the fully developed velocity profile at the channel input, the fRe values for the straight channel find an asymptotic behavior to the value of 61. The frictional coefficient is greater in the zigzag channels than in the straight channel due to the sharp edges in the fluid path.

Therefore, a periodic trend can be seen clearly in the Zigzag channels graph.

It is noteworthy that the frictional coefficient curve for the R=2 model is placed approximately on the straight channel frictional coefficient graph. Therefore, in addition to have a suitable heat transfer, this model also provides a better result in terms of hydraulic performance, since it has a lower pressure drop than other zigzag channels. The R=4 and R=8 models have the highest frictional coefficient values, which can be attributed to the physics of flow in these channels and the secondary flows that are formed along the broken arms of these channels, because the increased length of the broken arms and the consequent increase in the R will cause the back flows pass through a longer path and create greater drop. The next model is the R=1 model, where the frictional coefficients are in a wide range, because part of the flow passes through the center of the channel and a relatively straight path, which is resulting in less friction. However, the other part of the flow is enclosed in sharp edges and it has a rotational movement and more friction. Considering the examined cases, it can be concluded that the R=2 model has the best performance.

Since it is necessary to consider both the heat transfer and the pressure drop factors in designing a suitable cooling system in order to achieve an optimal case, it is better to use a graph in which the effect of the two factors has simultaneously been shown. For this purpose, the f/Nu graph is presented, which shows the ratio of frictional coefficient changes to the Nusselt number in Fig. 12. It is clear that the lower the value of this parameter, the better the

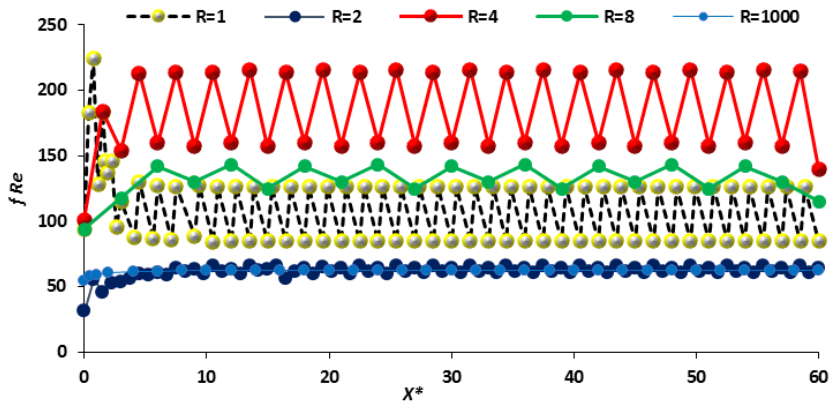

Fig.11. Evolution of the term fRe with the curvilinear coordinate for different channels

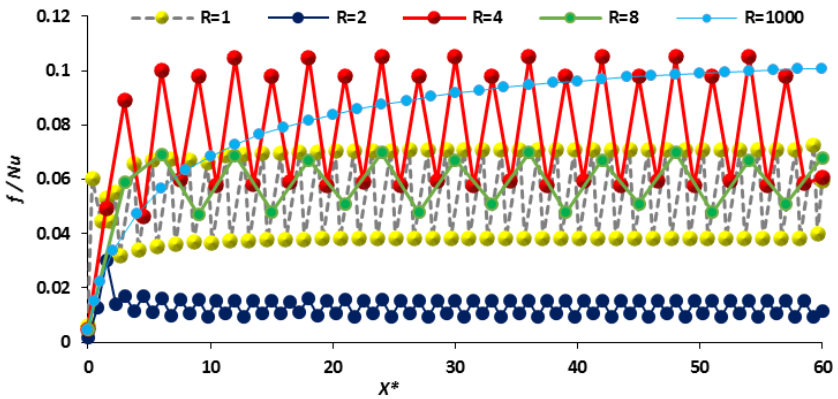

Fig.12. Evolution of the ratio of the friction factor to the Nusselt number with the curvilinear coordinate for different channels

channel performance. In most points, the f/Nu values for zigzag channels are less than those in the straight channel. On the other hand, with a movement along the channel, the f/Nu curve of the straight channel has an ascending trend and gets distant from the f/Nu curve of the zigzag channels that has a roughly uniform trend. In other words, as one moves forward the heat exchanger, the greater efficiency of chaotic mixing and its effect on heat transfer become more evident, and will achieve a lower f/Nu ratio than the non-chaotic model. Therefore, heat transfer increases more than the pressure drop in chaotic models.

In Fig. 12, the f/Nu curve of the R=2 geometry lies at the lowest level, after which the R=1 and R=8 geometries lie at higher levels. The values of f/Nu in the R=4 geometry are more volatile and these values, in some points, exceed the numbers which have been obtained for the straight channel as well.

5.Conclusion

This paper dealt with numerical simulation of the flow and heat transfer of a laminar which has been forced advection in a three-dimensional zigzag channel with rectangular cross sectional area under constant heat flux and compared the obtained results with the straight channel that commonly used in fuel cells. Moreover, the R-dimensionless parameter, which is the ratio of the length of each zigzag unit to the channel's width, was examined for the four values of R=1, 2, 4, and 8.

For this purpose, the existence of chaos in the flow for the zigzag channel under the examined conditions was approved based on the condition of sensitivity to the initial conditions. In addition, the path of particles with the help of Poincare mapping is traced, finding that the particles have a quite different path in the zigzag channel from R=2 onwards. Furthermore, examining the flow field showed that Dean Vortices have been formed in the zigzag channels, which occupy a greater part of the section of the channel in the R=2 geometry.

The local Nusselt number along the channel was used to examine the heat transfer rate of different channels and a significant increase was observed in the heat transfer rate in the zigzag channels. The best position belonged to the R=2 geometry, which had a mean Nusselt number of about 6.5 times as much as that of the straight channel. To examine the uniformity of temperature, which is an important factor in the proper functioning of the cell, the temperature profile was plotted in a certain section of all channels. The results indicated a more uniform and lower-temperature profile for zigzag geometries than the straight channel which has a parabolic profile. In addition, the two IUT and ΔT factors were used for the quantitative examination of the uniformity degree of temperature, again showing the better performance of zigzag channels, especially the R=2 geometry.

Then, the frictional coefficient along the channel was examined and it was found that its values for the R=2 geometry are roughly equal to those in the straight channel, while there was an increase in these values in other zigzag channels. This is due to the formation of vortex flows in the sharp corners of other zigzag models, which increases the intermolecular friction. To make a precise comparison between the changes in the Nusselt number and the frictional coefficient, the f /Nu ratio graph was plotted and it was observed that the mean value of this parameter was lower in the zigzag channels than in the straight channel and the R=2 geometry lied at the lowest level. As a result, heat transfer has had a greater increase than the pressure drop in the zigzag models.

The zigzag geometries have a chaotic advection flow from R=2 onwards and increase heat transfer as a result of a slight increase in pressure drop. The most appropriate model among the studied zigzag channels is the R=2 geometry, which is a confirmed geometry in terms of the thermal and hydraulic factors, and this chaotic model can be used as a compact heat exchanger for cooling the fuel cell of the polymer membrane.

References

[1] Asneghi A., Sarikhani N., Sadughi A. H., Kermani M. J., 3D Simulation and Product a 2 Watt Fuel Cell, in The 15th International Conference on Mechanical Ingineering, Tehran, Iran (2007).

[2] Ghafaritehrani A., Nozad A., Poornajadi A. B., Numerical Simulation of Fluid Flow in Gas Diffusion Layers and its Effect on PEMFC Efficiency, in The 1th National Conference on Hydrojen and Fuel cell, Tehran, Iran (2009).

[3] Chen F.C., Gao Z., Loutfy R.O., Hecht, M. Analyses of Optimal Heat Transfer in a

PEM Fuel Cell Cooling Plate, Fuel Cells (2003)3(4): 181–188.

[4] Lasbet Y., Auvity B., Castelain C., Peerhossaini H., A Chaotic Heat-Exchanger for PEMFC Cooling Applications, Power Sources (2006) 156(1): 114-118.

[5] Choi J., Kim Y.H., Lee Y., Lee K.J., Kim Y.C., Numerical Analysis on the Performance of Cooling Plates in a PEFC , Mechanical Science and Technology (2008) 22: 1417–1425.

[6] Yu S.H., Sohn S., Nam J.H., Kim C., Numerical Study to Examine the Performance of Multi-Pass Serpentine Flow-Fields for Cooling Plates in Polymer Electrolyte Membrane Fuel Cells, Power Sources (2009) 194: 697–703,.

[7] Dean W. R., Note on the Motion of Fluid in a Curved Pipe, The Philosophical Magazine (1927) 4: 208–223,.

[8] Wang L., Liu F., Forced Convection in Slightly Curved Micro Channels, International Journal of Heat and Mass Transfer (2007) 50(5–6): 881–896.

[9] Aref H., Stirring by Chaotic Advection, Journal of Fluid Mechanics (1984)143: 1–21.

[10] Wiggins S., Ottino J.M., Foundation of Chaotic Mixes (2004) 362: 937–970.

[11] Acharya N., Sen M., Chang H. C., Heat Transfer Enhancement in Coiled Tubes by Chaotic Mixing, Heat and Mass Transfer (1992) 35 (10) 2475-2489.

[12] Mokrani A., Castelian C., Peerhossaini H., The Effects of Chaotic Advection on Heat Transfer, Heat and Mass Transfer (1997) 40(13): 3089-3104.

[13] Xia H. M., Wang Z.P., Wan S. Y. M., Yin F.F., Numerical Study on Microstructured Reactor with Chaotic Heat and Mass Transfer and its Potential Application for Exothermic Process, Chemical Engineering Research and Design (2012) 90: 1719–1726.

[14] Senn S.M., Poulikakos D., Laminar Mixing, Heat Transfer and Pressure Drop in Tree-Like Micro Channel Nets and Their Application for Thermal Management in Polymer Electrolyte Fuel Cells, Power Sources (2004) 130: 178–191.

[15] Kuo J. K., Yen T. S., Chen C. K., Improvement of Performance of Gas Flow Channel in PEM Fuel Cells, Energy Conversion and Management (2008) 49: 2776–2787.

[16] Liu R.H., Stremler M.A., Sharp K.V., Olsen M.G., Santiago J.G., Adrian R.J., Aref H., Beebe D.J., Passive Mixing in a Three-Dimensional Serpentine Microchannel, Microelectromechanical Systems (2000) 9: 190–197.

[17] Gupta R., Geyer P. E., Fletcher D. F., Haynes B. S., Thermo Hydraulic Performance of a Periodic Trapezoidal Channel with a Triangular Cross-Section, Heat and Mass Transfer (2008) 51: 2925–2929.

[18] Sui Y., Teo C.J., Lee P.S., Chew Y.T., Shu C., Fluid Flow and Heat Transfer in Wavy Micro Channels, Heat and Mass Transfer (2010) 53: 2760–2772.

[19] Sui Y., Teo C.J., Lee P.S., Direct Numerical Simulation of Fluid Flow and Heat Transfer in Periodic Wavy Channels with Rectangular Cross-Sections, Heat and Mass Transfer (2012) 55: 73–88.

[20] Mengeaud V., Josserand J., Girault H.H., Mixing Processes in a Zigzag Micro Channel: Finite Element Simulation and Optical Study, Analytical Chemistry (2002) 74: 4279–4286.

[21] Zheng Z., Fletcher D. F., Haynes B. S., Transient Laminar Heat Transfer Simulations in Periodic Zigzag Channels, Heat and Mass Transfer (2014) 71: 758–768.

[22] Zheng Z., Fletcher D. F., Haynes B. S., Chaotic Advection in Steady Laminar Heat Transfer Simulations: Periodic Zigzag Channels with Square Cross-Sections, Heat and Mass Transfer (2013) 57: 274–284.

[23] Vinsard G., Dufour S., Saatdjian E., Mota J. P. B., Chaotic Advection and Heat Transfer in Two Similar 2-D Periodic Flows and in Their Corresponding 3-D Periodic Flows, Heat Mass Transfer (2016) 52: 521–530.

[24] Anxionnaz-Minvielle Z., Tochon P., Couturier R., Magallon C., Théron F., Cabassud M., Gourdon C., Implementation of 'Chaotic' Advection for Viscous Fluids in Heat Exchanger/Reactors, Chemical Engineering and Processing (2017) 113: 118–127.

[25] Bahiraei M., Mazaheri N., Alighardashi M., Development of Chaotic Advection in Laminar Flow of a Non-Newtonian

Nanofluid: A Novel Application for Efficient Use of Energy, Applied Thermal Engineering (2017) 124: 1213–1223.

[26] Marco S. M., Han L. S., A Note on Limiting Laminar Nusselt Number in Ducts with Constant Temperature Gradient by Analogy to Thin-Plate Theory, Heat Transfer (1955) 77: 625-630.

[27] Natarajan N. M., Lakshmanan S. M., Laminar Flow in Rectangular Ducts: Prediction of Velocity Profiles and Friction Factor, Indian Journal of Technology (1972) 10: 435-438.

[28] Spiga M., G.L. Morini, Nusselt Numbers in Laminar Flow for H2 Boundary Conditions, Heat and Mass Transfer (1996) 39: 1165–1174.

[29] Perng S. W., Wu H. W., Heat Transfer in a PEMFC Flow Channel, Applied Thermal Engineering (2009) 29: 3579–3594.

[30] Guo Z. Y., Li D.Y. , Wang B. X., A Novel Concept for Convective Heat Transfer Enhancement, International Journal of Heat and Mass Transfer (1998) 41: 2221–2225.

[31] Schmidt E., Properties of Water and Steam in SI-Units, Springer, New York (1989).

[32] Castelain C., Mokrani A., Le Guer Y., Peerhossaini H., Experimental Study of Chaotic Advection Regime in a Twisted Duct Flow the European Journal of Mechanics B Fluids (2001) 20: 205–232.

[33] Jiang F., Drese K. S., Hardt S., Küpper M., Schnfeld F., Helical Flows and Chaotic Mixing in Curved Micro Channels", AIChE (2004) 50: 2297–2305.

[34] Hobbs D. M., Muzzio F. J., Optimization of a Static Mixer Using Dynamical Systems Techniques, Chemical Engineering Science (1998) 53: 3199–3213.

[35] Aubin J., Fletcher D. F., Xuereb C., Design of Micromixers Using CFD Modeling, Chemical Engineering Science (2005) 60: 2503–2516.

[36] Ottino J. M., The Kinematic of Mixing: Stretching, Chaos and Transport, Cambridge University Press, New York (1989).